

Microstructure and High-Field Magnetic Properties of Fe-Based Bulk Amorphous Alloys

KATARZYNA BLOCH*

Institute of Physics, Faculty of Production Engineering and Materials Technology, Czestochowa University of Technology, 19 Armii Krajowej Str., 42-200 Czestochowa, Poland

In this paper the results of the structural and magnetic properties for bulk amorphous alloys Fe₆₅Co₁₀Y₃B₂₀ and Fe₆₃Co₁₀Y₇B₂₀ were presented. For the structural investigation was performed by X-ray diffractometry and Mossbauer spectroscopy. It was found that investigated samples were amorphous in the as-cast state. The magnetisation was measured within magnetic fields ranging from 0 to 2T using a vibrating sample magnetometer (VSM). On the basis of the hysteresis loops, the saturation magnetization value and the coercive field were determined. The investigation of the 'magnetisation in the area close to ferromagnetic saturation' showed that the magnetisation process in strong magnetic fields is connected with point defects and Holstein-Primakoff paraproces. Analysis of the high-field magnetization curves has facilitated the calculation of the spin wave stiffness parameter.

Keywords: bulk alloys, amorphous structure, Mossbauer spectroscopy, structural defects, Holstein-Primakoff paraproces

The functional materials, constituted by amorphous and nanocrystalline alloys, characterised with unique magnetic properties which result in the first place from their structure [1-12]. The structure of amorphous alloys is formed already in the process of their production [13-19]. Structural relaxations taking place during the production of amorphous alloys occur due to small displacements of atoms. They can accompany either the displacement of a single atom or a number of atoms, or the collective movement of a large quantity of atoms [20-37].

Structural relaxations are microscopic processes which lead to the change of both the structure and some macroscopic properties of amorphous materials. A proper tool to examine changes in an amorphous structure is Mossbauer spectroscopy. Structural relaxations can also be investigated by measuring magnetic properties of amorphous materials. One of the possible methods is the measurement of magnetization in high magnetic fields.

In strong magnetic fields, within the region known as the approach to the ferromagnetic saturation, the specimen does not reach the full saturation due to structural defects. These defects are sources of short-range stresses and as a result of magneto-elastic interaction between them and magnetization occurs a non-collinear magnetic structure. Magnetization (M) of an amorphous alloys in a strong magnetic field (H) can be described by the equation [37-39]:

$$\mu_0 M(H) = \mu_0 M_s \left(1 - \sum_{n=1}^4 a_{n/2} / \mu_0 H^{n/2} \right) + \chi \mu_0 H + b(\mu_0 H)^{1/2} \quad (1)$$

where:

- M_s - saturation magnetization;
- $a_{n/2}$, b coefficients;
- χ - magnetic susceptibility;
- μ_0 - magnetic permeability of the vacuum;
- $a_{n/2} / \mu_0 H^{n/2}$ - the term expressing the influence of structural defects;
- $\chi \mu_0 H$ - the term resulting from paramagnetism of electron band and diamagnetism of complete atomic shells;

$b(\mu_0 H)^{1/2}$ - expression - determining an increase in magnetization due to damping of the spin-waves by the magnetic field.

The term $a_{1/2} / (\mu_0 H)^{1/2}$ is related with the point defects, and described as follows:

$$\frac{a_{1/2}}{(\mu_0 H)^{1/2}} = \mu_0 \frac{3}{20 A_{ex}} \left(\frac{1+\nu}{1-\nu} \right)^2 \times G^2 \lambda_s^2 (\Delta V)^2 N \left(\frac{2 A_{ex}}{\mu_0 M_s} \right)^{1/2} \frac{1}{(\mu_0 H)^{1/2}} \quad (2)$$

where:

- A_{ex} - exchange constant;
- ν - Poisson's ratio;
- G - shear modulus,
- λ_s - saturation magnetostriction;
- ΔV additional specimen volume related to point defects,
- N - volume density of point defects.

The terms $a_1 / \mu_0 H$ and $a_2 / (\mu_0 H)^2$ are related to the linear defects. When the dominant role plays the term $a_1 / \mu_0 H$ equation (1) takes the form of the second law of approach to the ferromagnetic saturation:

$$\frac{a_1}{\mu_0 H} = 1,1 \mu_0 \frac{G^2 \lambda_s^2}{(1-\nu)^2} \frac{N b_{eff}}{M_s A_{ex}} D_{dip}^2 \frac{1}{\mu_0 H} \quad (3)$$

If the term $a_2 / (\mu_0 H)^2$ is dominant, it can be expressed by the equation:

$$\frac{a_2}{\mu_0 H^2} = 0,456 \mu_0 \frac{G^2 \lambda_s^2}{(1-\nu)^2} \frac{N b_{eff}}{M_s^2} D_{dip}^2 \frac{1}{(\mu_0 H)^2} \quad (4)$$

Then the form of the equation (1) comes down to the third law of approach to the ferromagnetic saturation.

For high values of magnetic fields, above the range where the relationships involving the influence of structural defects are valid, a further slight increase in magnetization proceeds according to the term $b(\mu_0 H)^{1/2}$, describing the Holstein-Primakoff paraproces [40, 41].

Coefficient b is related to the spin-wave stiffness parameter D_{sp} by the formula [42, 43]:

* email: 23kasia1@wp.pl

$$b = 3,54 g \mu_0 \mu_B \left(\frac{1}{4\pi D_{sp}} \right)^{3/2} kT (g \mu_B)^{1/2} \quad (5)$$

where:

g - Lande splitting factor;

μ_B - Bohr magneton.

The aim of the work was to examine the structure and magnetic properties of the bulk $\text{Fe}_{65}\text{Co}_{10}\text{Y}_5\text{B}_{20}$ and $\text{Fe}_{65}\text{Co}_{10}\text{Y}_7\text{B}_{20}$ alloys, and in particular to determine the type of structural defects found in the tested materials.

Computational details

The samples used in the investigations were made using high purity elements: Fe-99.99%, Co-99.98%, and Y-99.98%. The element boron was added in the form of $\text{Fe}_{45.4}\text{B}_{54.6}$ alloy. The samples were produced in the form of rods, of diameter 1 mm and length 1 cm, using an injection casting method.

The materials structures were investigated using X-ray diffractometry and Mossbauer spectroscopy. XRD patterns and Mossbauer spectra were recorded for powdered test samples, since this allows the gathering of information about the underlying structure of the entire alloy volume. The BRUKER X-ray diffractometer was equipped with a lamp with a cobalt source. Investigations were carried out over the 2Θ range from 30 to 120° , with a measurement step of 0.02° and the time per step of 5 s. The transmission Mossbauer spectra were measured at room temperature using conventional Mossbauer spectrometer working at a constant acceleration with a ^{57}Co (Rh) radioactive source of the 70 mCi in activity.

Measurement of magnetization as a function of magnetic field induction in strong magnetic fields was done using a vibration magnetometer (LAKE SHORE model 7301) in the range of 0 to 2 T. From the analysis of the static hysteresis loops, parameters such as the saturation magnetization and the coercivity were found. The results of the magnetic investigations, carried out in both weak and strong magnetic fields, were interpreted according to the Kronmuller theorem. This allowed for verification of the underlying microstructure of the alloys.

Results and discussions

X-ray diffraction images for the investigated samples in the as-quenched state are presented in figure 1.

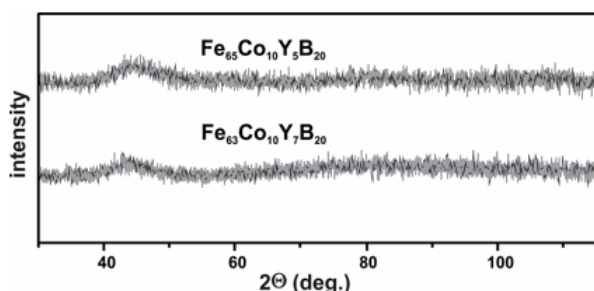


Fig. 1. X-ray patterns obtained for examined materials [44]

The resulting X-ray diffraction images are characteristic of amorphous materials. They show a wide maximum occurring at the angle of $2\Theta \approx 44^\circ$, which is characteristic of the amorphous structure.

Amorphicity of the tested alloys confirmed the results of the Mossbauer research.

Figure 2 shows the Mossbauer transmission spectra recorded for the tested alloys.

The Mossbauer transmission spectra of the examined specimens consist of broad asymmetric overlapping lines, what is typical for spectra achieved for amorphous

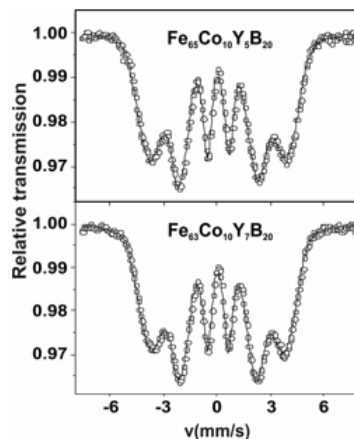


Fig. 2. Mossbauer transmission spectra recorded for the tested alloys [45]

materials. From the Mossbauer spectra of the amorphous samples the hyperfineubartsch method (fig. 3) [46, 47].

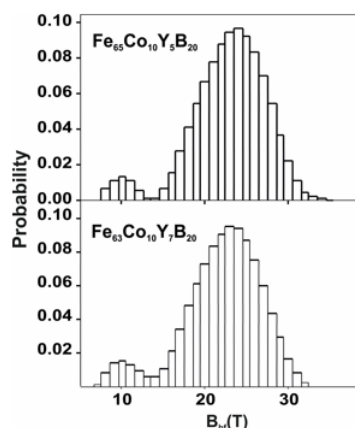


Fig. 3. Corresponding hyperfine field distributions of the bulk amorphous alloys [45]

In the hyperfine field distribution $P(B)$ obtained from these spectra one can distinguish at least two components related to the regions with the different iron concentration. Based on numerical calculations based on hyperfine field distributions, it was found that the value of the mean hyperfine box index for investigated alloys is equal to: 22.79 T for $\text{Fe}_{65}\text{Co}_{10}\text{Y}_5\text{B}_{20}$ and 22.08 T for $\text{Fe}_{65}\text{Co}_{10}\text{Y}_7\text{B}_{20}$, respectively. The mean value of the hyperfine field induction decreases with Y concentration because the magnetic structure becomes more and more non-collinear due to the exchange interaction fluctuations in the magnitude and sign [48, 49].

Figure 4 shows the static magnetic hysteresis loops measured for tested alloys.

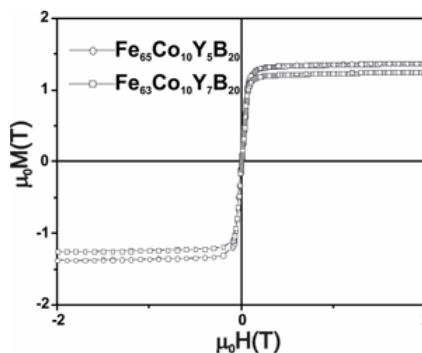


Fig. 4. Static hysteresis loops obtained for the investigated alloys

Magnetic examinations were performed by means of a vibrating sample magnetometer and revealed that static hysteresis loop recorded for the examined specimens had typical shapes found for magnetic materials of the so-called soft magnetic properties [50, 51]. The measurements were a basis for determination of the saturation magnetization and the coercive field values (table 1).

Table 1
PARAMETERS OBTAINED FROM THE ANALYSIS OF STATIC HYSTERESIS LOOPS: M_s - SATURATION MAGNETIZATION, H_c - COERCIVE FIELD

| Parameters | M_s (T) | H_c (A/m) |
|---------------------------|-----------|-------------|
| Samples | | |
| $Fe_{65}Co_{10}Y_5B_{20}$ | 1.37 | 31.8 |
| $Fe_{63}Co_{10}Y_7B_{20}$ | 1.25 | 38.2 |

The value of saturation magnetization is greater for the $Fe_{65}Co_{10}Y_5B_{20}$ than the second alloy. This result is consistent with the results obtained with the Mossbauer spectroscopy (greater value of B_{hf} parameter). The higher value of these parameters indicates the greater atomic packing density in the $Fe_{65}Co_{10}Y_5B_{20}$ material.

In figure 5 the curves of relative magnetization M/M_s versus induction of magnetizing field for the amorphous $Fe_{65}Co_{10}Y_5B_{20}$ and $Fe_{63}Co_{10}Y_7B_{20}$ alloys are shown.

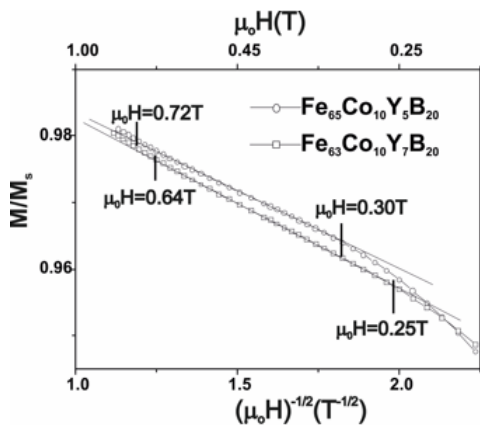


Fig. 4. The high-field magnetization curves $M/M_s((\mu_0H)^{-1/2})$ for investigated alloys

The linear dependence of $\mu_0 M((\mu_0H)^{-1/2})$ within the magnetic field range of: 0.30 T-0.72 T for $Fe_{65}Co_{10}Y_5B_{20}$ and 0.25 T-0.64 T for $Fe_{63}Co_{10}Y_7B_{20}$ confirms that the magnetization process for both investigated alloys is connected with rotation of the magnetization vector in the vicinities of the point defects [52, 53].

In strong magnetic fields, i.e. $\mu_0H > 0.72$ T for $Fe_{65}Co_{10}Y_5B_{20}$ alloy and $\mu_0H > 0.64$ T for $Fe_{63}Co_{10}Y_7B_{20}$ alloy, respectively, the Holstein-Primakoff paraproces was observed (fig. 5) [52].

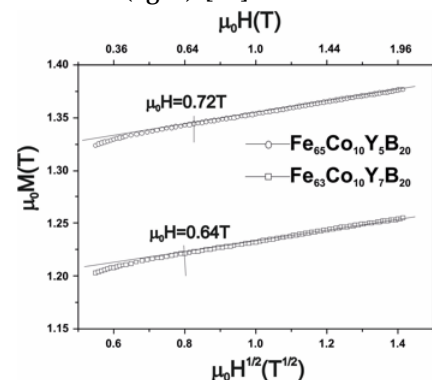


Fig. 5. The high-field magnetization curves $\mu_0M((\mu_0H)^{1/2})$ for investigated alloys

The parameters obtained from the analysis of the high-field magnetization curves are presented in table 2.

The analysis of the high-field magnetization curves in the Holstein-Primakoff paraproces range enabled determination of the spin wave stiffness parameter D_{sp} [41-44]. The value of this parameter is similar for a both investigated alloys.

Table 2
EXPERIMENTAL VALUES OF THE PARAMETERS: $a_{1/2}$, b AND THE STIFFNESS PARAMETER OF THE SPIN WAVE D_{sp}

| Parameters | $a_{1/2}$ (T ^{-1/2}) | b (T ^{1/2}) | D_{sp} [10 ⁻² eVnm ²] |
|---------------------------|--------------------------------|-------------------------|------------------------------------------------|
| Samples | | | |
| $Fe_{65}Co_{10}Y_5B_{20}$ | 0.0238 | 0.056 | 45 |
| $Fe_{63}Co_{10}Y_7B_{20}$ | 0.0255 | 0.055 | 46 |

Conclusions

Investigated alloys obtained by the injection casting method are fully amorphous. However, they are not homogeneous and in the hyperfine field distributions at least two components corresponding to the regions with different iron concentration can be distinguished. The average magnetic hyperfine field induction decreases with Y content.

On the basis of virgin magnetisation curve analysis, the type of structural defects occurring in the investigated samples were determined. In the case of both alloys the point-like defects influence the magnetization in high magnetic fields. In the magnetic field $\mu_0H > 0.72$ T and $\mu_0H > 0.64$ T for $Fe_{65}Co_{10}Y_5B_{20}$, $Fe_{63}Co_{10}Y_7B_{20}$ alloys, respectively, the Holstein-Primakoff paraproces is observed. Analysis of the initial magnetization curve in paraproces region allows the determination of a parameter describing the stiffness of the spin wave (D_{sp}).

On the basis of the performed investigations it can be stated that the $Fe_{65}Co_{10}Y_5B_{20}$ characterized by a greater packing density of atoms (larger value B_{hf} , M_s).

References

- INOUE A, GOOK J. S., Mater. Trans. JIM 36, 1995, pp. 1180-1183.
- NABIALEK M., Arch. Metall. Mater.61, 2016, pp. 445-450
- INOUE A., KATSUYA A., Mater. Trans. JIM 37, 1996, pp. 1332-1336
- INOUE A., ZHANG T., ITOI T, TAKEUCHI A., Mater. Trans. JIM 38, 1997, pp. 359-362.
- INOUE A., KOSHIBA H., ITOI T, MAKINO A., Appl. Phys. Lett. 73, 1998, pp. 744-746.
- GEBARA P, KOVAC J., Mater. Des., 129, 2017, pp. 111-115.
- GEBARA P, PAWLK P, HASIAK M., J. Magn. Magn. Mater., 422, 2017, pp. 61-67.
- GEBARA P, KOVAC J., J.Magn. Magn. Mater., 454, 2018, pp. 298-303.
- GEBARA P, Rare Met., DOI 10.1007/s12598-017-0917-6
- NABIALEK M., J. Alloys Comp., 642, 2015, pp. 98-103
- GRUSZKA K., NABIALEK M., BLOCH K., OLSZEWSKI J., Nukleonika 60, 2015, pp. 23-27
- INOUE A., Mater. Sci. Foundations 6, 1998, TRANSTECH PUBLICATIONS
- INOUE A., Mat. Sci. Eng., 226-228, 1997, pp. 357-363
- GONDRO J., BLOCH K.,NABIALEK M., GARUS S., Material. tehnologije, 50 (4), 2016, pp. 559-564
- GARUS S., NABIALEK M., BLOCH K., GARUS J., Acta Phys. Pol., 126, 2014, pp.997
- PIETRUSIEWICZ P., NABIALEK M., Acta Phys. Pol. A, 131 nr 4, 2017, pp. 678
- PIETRUSIEWICZ P., NABIALEK M., Acta Phys. Pol. A, 130 nr 4, 2016, pp. 920
- GONDRO J., J. Magn. Magn. Mater., 432, 2017, p. 501-506
- GRUSZKA K., Materiali in tehnologije/Materials and technology 50, 2016, pp.707-718
- TAKAHARA Y., Mat. Sci. Eng., A231, 1997, pp. 128-133
- MARZO F. F., PIERNA A. R., VEGA M. M., J. Non-Cryst. Solid., 329, 2003, pp. 108-114
- KHONIK S. V., KAVERIN L. D., KOBALOV N. P., NGUYEN N. T. N., LYSENKO A. V., YAZVITSKY M. YU., KHONIK V. A., J. Non-Cryst. Solid., 354, 2008, pp. 3896-3902

23. HARUYAMA O., SAKAGAMI H., NISHIYAMA N., INOUE A., *Mat. Sci. Eng.*, A 449-451, 2007, pp. 497-500
24. WANG X. D., JIANG J. Z., YI S., *J. Non-Cryst. Solid.*, 353, 2007, pp. 4157-4161
25. PIETRUSIEWICZ P., K. BLOCH., NABIAAEK M., WALTERS S., *Acta Phys. Pol. A*, 127 no 2, 2015, pp. 397-399
26. BŁOCH K., NABIALEK M., *Acta. Phys. Pol. A*, 127, 2015, pp. 442-444
27. RZYCKI K., BLOCH K., WALTERS S., *Acta. Phys. Pol. A*, 131, 2017, pp. 720-722
28. PIETRUSIEWICZ P., NABIALEK M., OLSZEWSKI J., LESZ S., *Material. tehnologije*, 51, 2017, pp. 157-162
29. TANASE, S.I., TANASE, D., SANDU, A.V., GEORGESCU, V., *Journal Of Superconductivity And Novel Magnetism*, 25, no. 6, 2012, p. 2053.
30. POIANA, M., DOBROMIR, M., NICA, V., SANDU, I., GEORGESCU V., *Journal Of Superconductivity And Novel Magnetism*, 26, no. 10, 2013, p. 3105.
31. PAPADATU, C.P., SANDU, A.V., BORDEL, M., SANDU, I.G., *Rev. Chim. (Bucharest)*, **68**, no. 4, 2017, p. 675.
32. TANASE, S.I., TANASE, D., DOBROMIR, M., SANDU, A.V., GEORGESCU, V., *Journal Of Superconductivity And Novel Magnetism*, 29, no. 2, 2016, p. 469.
33. GRIMBERG, R., UDPA, L., SAVIN, A., STEIGMANN, R., VIZUREANU, P., BRUMA, A., UDPA, S.S.,
34. *** *Research In Nondestructive Evaluation*, 19, no. 4, 2008, p. 202.
35. BINDEA, M., CHEZAN, C.M., PUSKAS, A., *Journal Of Applied Engineering Sciences*, 5, no. 1, 2015, p. 7.
36. VIZUREANU, P., *Metalurgia International*, 14, no. 5, 2009, p. 5.
37. VIZUREANU, P., AGOP, M., *Materials Transactions*, 48, no. 11, 2007, p. 3021.
38. KRONMULLER H., *IEEE Trans. Magn.*, 15, 1979, pp. 1218-1225
39. KRONMULLER H., ULNER J., *J. Magn. Magn. Mater.* 6, 1977, pp.52-56
40. KRONMULLER H., *J. Appl. Phys.* 52, 1981, pp.1859-1864
41. HOLSTEIN T., PRIMAKOFF H., *Phys. Rev.* 58, 1940, pp. 1098-1113
42. BLOCH K., NABIALEK M., *Acta. Phys. Pol. A* 127, 2015, pp. 413-414
43. KOHMOTO O., *J. Appl. Phys.* 53, 1982, pp.7486-7490
44. VASQUEZ M., FERNENGEL W., KRONMULLER H., *Phys. Stat. Sol.*, 115, 1989, pp.547
45. BLOCH, K., TITU, M. A., SANDU, A. V., *Rev. Chim. (Bucharest)*, **68**, no. 9, 2017, p. 2162
46. BRAND R. A., *Nuclear Instruments and Methods in Physics Research B*, 28, 1987, pp. 398-416
47. HESSE J., RUBARTSCH A., *J. Phys. E: Scientific Instruments*, 7, 1974, pp. 526-532
48. COEY J.M.D., GIVORD D., LIENARD A., REBOUILLAT J.P., *J. Phys. F: Metal Phys.* 11, 1981, pp. 2707-2725
49. CHAPPERT J., COEY J.M.D., LIENARD A., REBOUILLAT J.P., *J. Phys. F: Metal Phys.*, 11, 1981, pp. 2727-2744
50. BLOCH K., NABIALEK M., SZOTA M., *Rev. Chim. (Bucharest)*, **68**, no. 1, 2017, p. 18
51. NABIALEK M.G., PIETRUSIEWICZ P., DOSPIAL M.J., SZOTA M., BŁOCH K., GRUSZKA K., OGA K., GARUS S., *Journal of Alloys and Compounds*, 615, 2014, pp. S51-S55
52. SZOTA M., *Arch. Metall. Mater.* 60 (4), 2015, p. 3095-3100
53. SOB CZYK K., ZBROSZCZYK J., NABIALEK M., OLSZEWSKI J., BRYGIEL P., CEWIERCZEK J., CIURZYNSKA W., LUKIEWSKA A., LUBAS M., SZOTA M., *Arch. Metall. Mater.* 53, 2008, pp. 855-860

Manuscript received: 3.12.2017